Study on Pulsed Plasma Thruster Configuration to Expand Impulse Bit Range

IEPC-2005-234

Junji Uezu* and Junpei Iio*
Tokyo Metropolitan Institute of Technology (presently, Tokyo Metropolitan University)
Asahigaoka 6-6, Hino, Tokyo, 191-0065, Japan

Yukiya Kamishima* and Haruki Takegahara†
Tokyo Metropolitan University, Asahigaoka 6-6, Hino, Tokyo, 191-0065, Japan

Takashi Wakizono‡
HI-SERVE Corporation, Totohara 780-7, Akiruno, Tokyo, 190-0152, Japan

and

Mitsuteru Sugiki§
Astro Research Corporation, Godo-cho 134, Hodogaya-ku, Yokohama, Kanagawa, 240-0005, Japan

Abstract: In this study, the coaxial PPTs with Teflon cavity were developed to aim the large impulse bit, and the influences of its cavity configurations and the stored energy on the thrust performance were investigated. As a result, it became evident that larger impulse bit with lower specific impulse was generated at smaller cavity diameter and/or longer cavity length. And the maximum impulse bit of 2.5 mNs was generated at the stored energy of 28 J, then, the specific thrust achieved 90 μN/W. As a result, in addition to the rectangular PPTs that have been researched in TMIT, the PPT that generates larger impulse bit was established with almost same dimension (approximately 50×50×100 mm), weight (less than 2 kg), and power consumption (less than 30 W). By using these PPTs, a very wide range of the thrust performance, from the impulse bit of 1.5 mNs with the specific impulse of 360 s to the impulse bit of 90 μNs with the specific impulse of 1900 s, were achieved.

Nomenclature

C = capacitance
d = cavity diameter
E_0 = stored energy in the capacitors
E_{loss} = lost energy in the each resistor
E_{in} = supplied energy to the thruster head
E_t = utilized energy to the plasma acceleration
I_b = impulse bit
I_{sp} = specific impulse
J = main discharge current
L = inductance of the main discharge circuit
ℓ = cavity length
Q = stored electric charge in capacitors
R = resistance of the main discharge circuit
S = ablation area of the propellant
V = charged voltage in capacitors
Δm = mass shot of the propellant
η_t = thrust efficiency
η_{acc} = acceleration efficiency
η_{tr} = transfer efficiency
ω = angular frequency of the main discharge current

Subscripts with L and R
0 = value at the beginning of the discharge
tot = total
c = capacitors
p = plasma
t = transmission lines including the electrodes

* Master's Course, Department of Aerospace Engineering, ppt@astak3.tmit.ac.jp
† Professor, Department of Aerospace Engineering, hal@astak3.tmit.ac.jp
‡ President, wakizon@kch.biglobe.ne.jp
§ President, sugiki@astro-r.co.jp

I. Introduction

The Pulsed Plasma Thruster (PPT) is one of the promising electric propulsion system, which has the following advantages; 1) it has a simple structure and is a lightweight by using solid propellant like polytetrafluoroethylene (PTFE), 2) it generates the small impulse bit at optional time interval, thus a control of the total impulse is easy, 3) it operates with low power consumption[1]. In Tokyo Metropolitan Institute of Technology (TMIT), the rectangular and breech-fed PPT (PPT-B20) has been researched and developed as the propulsion system for a small satellite[2,3]. The photograph and the thrust performance of its system are shown in Fig. 1 and Table 1[4], respectively. It generates the very small impulse bit of 22 μNs with the high specific impulse of 960 s. And the power consumption of its system is only 4.2 W at 1 Hz operation. Therefore, PPT-B20 is appropriate for the missions that demand a precise total impulse and a long life. On the other hand, its impulse bit is little too small to comply with the missions such as a formation flying and an orbit transfer, that demand a large impulse bit and a high ΔV. Therefore in addition to PPT-B20, the PPT that generates a large impulse bit has been expected for application to such various missions.

In this study, the several configurations of the thruster head had been examined to aim a large impulse bit[5], and the evaluations on the coaxial PPTs that generate largest impulse bit are described in detail. In general, there are some configurations in the coaxial PPTs[6,7], the type with Teflon cavity was employed to expect larger impulse bit.

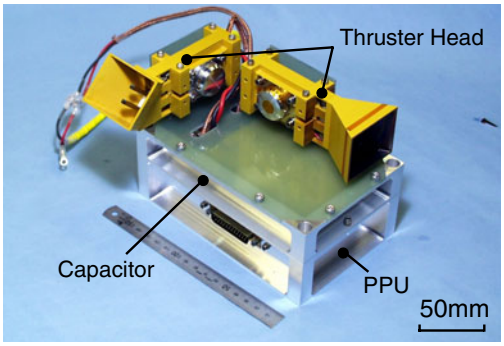

Fig. 1 Photograph of PPT-B20 system.

Table 1 Thrust performance of PPT-B20.

Items	Specifications
Capacitance, μ F	3.0
Charged Voltage, kV	1.5 (Nominal)
Stored Energy, J	3.3 (Nominal)
Power Consumption, W	4.2 (Nominal)
Impulse Bit, μ Ns	22
Mass Shot, μ g/shot	2.3
Specific Impulse, s	960
Thrust Efficiency, %	3.1
Specific Thrust, μ N/W	6.5

II. Objectives

The objectives of this study are as follows.

In order to broaden the range of PPT thrust performance,

1) to evaluate the influences of the stored energy and the cavity configurations on the thrust performance, using the coaxial PPT with Teflon cavity,
2) to investigate achievable thrust performance range, using the rectangular PPTs that have been researched in TMIT as well as the coaxial PPT.

Furthermore, in order to clarify the internal phenomenon of the coaxial PPT,

3) to investigate the characteristics of the main discharge circuit and the energy distribution of the stored energy.

III. Experimental Apparatus and Procedure

A. Thruster Heads

A-1. PPT-Co

Figures 2 and 3 show the photograph and a cross-section view of PPT-Co, respectively. As shown in these figures, the solid anode, made of Aluminum, and the cylindrical cathode, made of Brass were arranged at the upstream and the downstream position with the same axis, respectively. The propellant is the cylindrical PTFE, and the cathode has a divergent nozzle. The inner diameter of the cylindrical PTFE is defined as the cavity diameter d, and a distance between the anode tip and the cathode is also defined as the cavity length ℓ. Additionally, the ablation area S is defined as the inner surface of the cylindrical PTFE as the following equation:

$$S = \pi dl \tag{1}$$

The cavity diameter (same as the cathode inner diameter) is 3 mm, smaller than that of the conventional coaxial PPTs[6,8], and the cavity length is 20 mm. The ignitor is common to that of PPT-B20.

A-2. PPT-CoII

The cross-section view of PPT-CoII is shown in Fig. 4. Compared with PPT-Co, PPT-CoII does not have divergent nozzle on the cathode and the anode is made of Brass. Furthermore in PPT-CoII, the cavity diameter and the cavity length were variable by replacing the propellant and both electrodes. The cavity diameter was varied from 3 mm to 10 mm, and the cavity length was varied from 10 mm to 50 mm, respectively. These two thruster heads are almost same in other design.

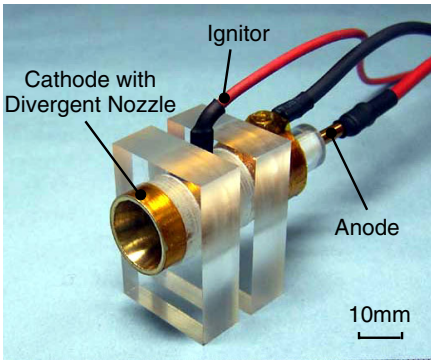

Fig. 2 Photograph of PPT-Co.

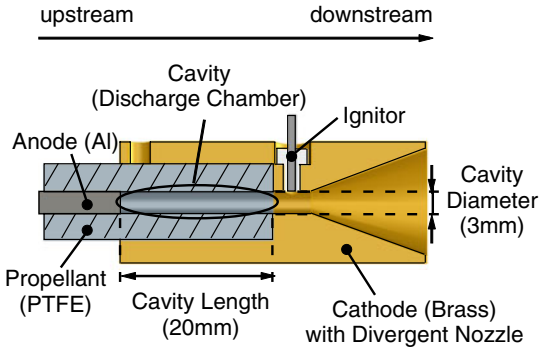

Fig. 3 Cross-section view of PPT-Co.

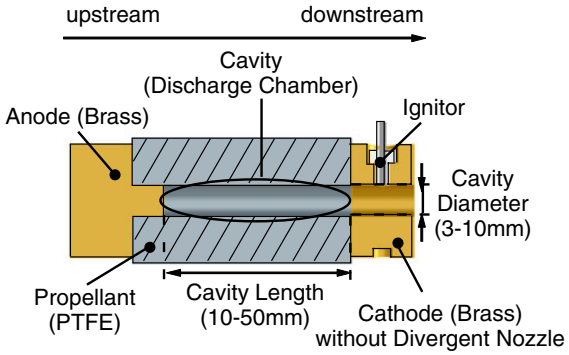

Fig. 4 Cross-section view of PPT-CoII.

B. Thrust Performance and Main Discharge Current

In this study, the impulse bit I_b, the mass shot Δm, the specific impulse I_{sp}, and the thrust efficiency η_t were obtained as the thrust performance. The impulse bit was measured by a target method, and the mass shot was calculated by averaging the total mass loss through the repetitive operation. Furthermore, the specific impulse and the thrust efficiency were calculated by the following equations, respectively:

$$I_{sp} = I_b / (\Delta m \cdot g) \tag{2}$$

$$\eta_t = I_b^{\,2} / (2\Delta m \cdot E_0) \tag{3}$$

where g and E_0 are gravity acceleration and the stored energy in capacitors, respectively.

And the main discharge currents were obtained to investigate the inductance and the resistance of the main discharge circuit. These were measured by a Rogowski coil, just after the impulse bit measurement.

C. Experimental Conditions

C-1. Vacuum Facility

All experiments were conducted in a vacuum chamber, and its diameter and length are 0.9 m and 2.1 m, respectively. Through a PPT operation, a pressure in the vacuum chamber was kept at approximately 6×10^{-3} Pa.

C-2. Tests Using PPT-Co

In the tests using PPT-Co, two experiments were conducted at the conditions as shown in Table 2. One of the experiments was the thrust performance measurement, and the other was the impulse bit range measurement. The

Table. 2 Experimental conditions with PPT-Co.

Items	Thrust Performance Measurement	Impulse Bit Range Measurement
Parameters	Stored Energy	Stored Energy
Measured Performance	Impulse Bit and Mass Shot	Only Impulse bit
Capacitance, μ F	6.2	6.2
Charged Voltage, kV	1.0, 1.8	0.4 - 3.0
Stored Energy, J	3.1, 10	0.5 - 28
Cavity Diameter, mm	3	3
Cavity Length, mm	20	20
Length / Diameter (ℓ/d)	6.7	6.7
Ablation Area, cm^2	1.9	1.9
Energy Density, J/cm^2	1.6, 5.3	0.3 - 15

Table. 3 Experimental conditions with PPT-CoII.

Items	Thrust Performance Measurement		Impulse Bit Range Measurement
Parameters	Stored Energy	Cavity Configuration	Stored Energy and Cavity Configuration
Measured Performance	Impulse Bit and Mass Shot	Impulse Bit and Mass Shot	Only Impulse bit
Capacitance, μ F	4.7, 13.8	13.8	9.2
Charged Voltage, kV	1.2, 1.6, 2.0	1.2	0.6 - 2.8
Stored Energy, J	3.4, 10, 18, 28	10	1.6 - 36
Cavity Diameter, mm	3	3, 5, 8,10	3, 5, 8
Cavity Length, mm	20	10, 20, 30, 50	10, 20, 50
Length / Diameter (ℓ/d)	6.7	1.0 - 17	1.3 - 17
Ablation Area, cm^2	1.9	0.9 - 16	1.6 - 7.9
Energy Density, J/cm^2	1.8 - 15	0.6 - 11	0.8 - 23

objective of the former experiment was to investigate the difference of the thrust performance due to the stored energy. The impulse bit and the mass shot were measured at the stored energy of 3.1 J and 10J, and the mass shot was averaged by approximately 1000 shots operation. Furthermore, the specific impulse and the thrust efficiency were calculated by Eqs. (2) and (3), respectively. And the objective of the latter experiment was to investigate the achievable impulse bit range by varying the only stored energy. And the impulse bit was measured at the stored energy from 0.5 J to 28 J.

C-3. Tests Using PPT-CoII

In the test using PPT-CoII, two experiments were also conducted at the conditions as shown in Table 3. One of the experiments was the thrust performance measurement, and this experiment was subdivided into two conditions. And the other was the impulse bit range measurement. The objective of the former experiment was to investigate the difference of thrust performance due to the stored energy and the cavity configuration. In the case of evaluation of the stored energy on the thrust performance, the stored energy was varied from 3.4 J to 28 J, the cavity configuration was kept at the diameter of 3 mm and the length of 20mm. On the other hand, when the cavity configuration were investigated, the cavity diameter was varied from 3 mm to 10 mm, and the cavity length was varied from 10 mm to 50 mm, respectively, and the stored energy was kept at 10 J. All combinations of the cavity diameter and its length, shown in Table 3, were examined. The impulse bit and the mass shot were measured at the above each experimental condition, and the mass shot was averaged by approximately 500 shots operation in these two experiments. And the objective of the latter experiment was to investigate the achievable impulse bit range by varying the stored energy and the cavity configuration. The impulse bit was measured by varying the stored energy and the experimental condition as shown in Table 3.

IV. Results and Discussions

A. Results of Thrust Performance Measurement

A-1. Effects of Stored Energy

The thrust performance by varying the stored energy was obtained with PPT-Co and PPT-CoII. As shown in Fig. 5, it was arranged by the energy density defined as the ratio of the stored energy to the ablation area. It was confirmed that the impulse bit and the mass shot were linearly proportional to the energy density. On the other hand, the specific impulse and the thrust efficiency were almost constant with the increase of the energy density.

A-2. Effects of Cavity Configuration

The impulse bit and the specific impulse by varying the cavity configurations with PPT-CoII were shown in Fig. 6, arranged by the cavity length. In the cases that the cavity diameter was 8 or 10 mm and its length was 50mm, the repetitive operation of 500 shots had not been achieved due to the charring on inner surface of the cylindrical PTFE. As the cause of this charring, an insufficiency of the energy supplied to the PTFE is considered. Because the ablation areas of those two configurations were larger than those of other configurations, thus these energy density became low value of 0.8 J/cm^2 or 0.6 J/cm^2, respectively. The repetitive operation was achieved when the energy density was more than approximately 1.1 J/cm^2. So it is considered that the energy density for successful repetitive operation is required the following inequality roughly:

$$E_0 / S \geq 1.0 \ [J/cm^2] \tag{4}$$

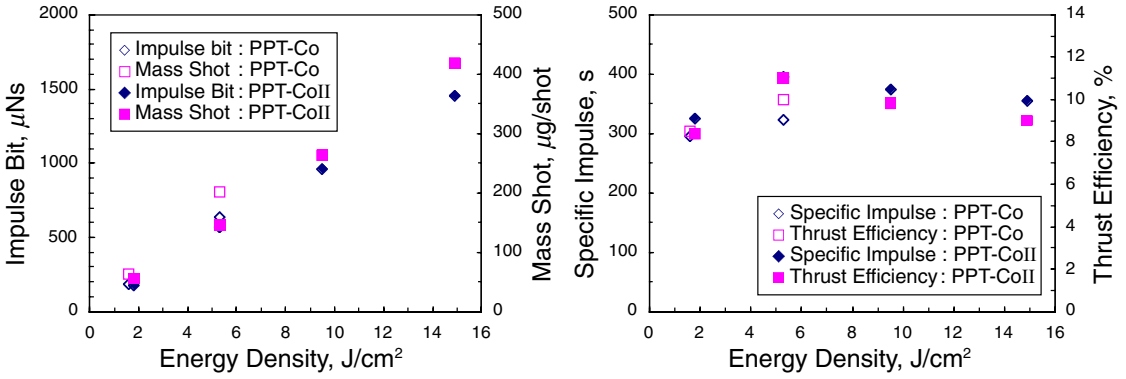

a) Impulse bit and mass shot arranged by energy density

b) Specific impulse and thrust efficiency arranged by energy density

Fig. 5 Thrust performance by varying stored energy (d =3mm, ℓ =20mm, i.e. S =1.9cm^2).

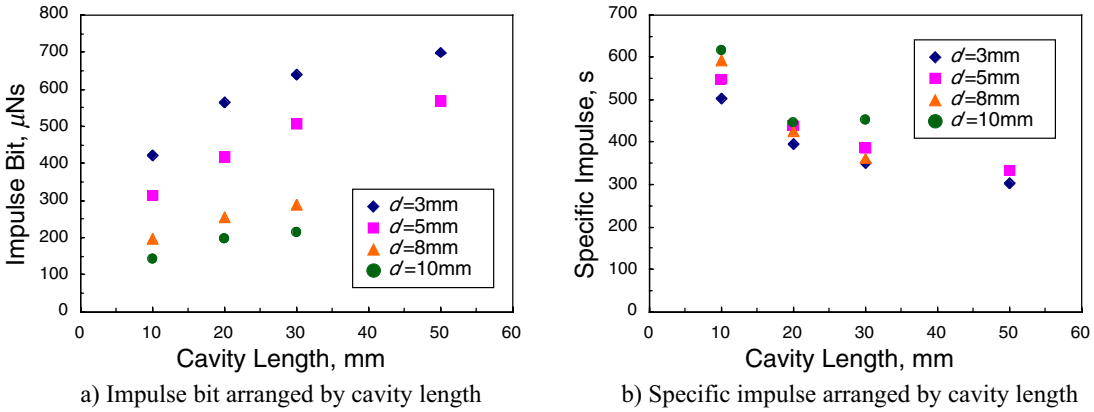

a) Impulse bit arranged by cavity length

b) Specific impulse arranged by cavity length

Fig. 6 Thrust performance by varying cavity configurations (E_0=const=10J).

As shown in Fig. 6, it was confirmed that as the cavity length increased, the impulse bit increased and the specific impulse decreased, respectively. Furthermore, the larger impulse bit was generated at the smaller cavity diameter, and the higher specific impulse was obtained at the larger cavity diameter.

A-3. Thrust Performance Range with Coaxial PPT at Same Stored Energy

The thrust performance achieved with PPT-Co and PPT-CoII at the constant energy of 10 J is shown in Fig. 7. And the values of ℓ/d are constant on each linear solid lines listed in Fig. 7. It is confirmed that a wide range of the thrust performance is achieved by varying only the cavity configurations, and the maximum impulse bit is 700 μNs with the specific impulse of 300 s at the ℓ/d of 17, and the maximum specific impulse is 620 s with the impulse bit of 140 μNs at the ℓ/d of 1.0.

Furthermore, the impulse bit is also indicated as follows by using Eqs. (2) and (3):

$$I_b = \frac{2\eta_t E_0}{gI_{sp}} \tag{5}$$

When the thrust efficiency and the stored energy are assumed as constant in Eq. (5), the impulse bit becomes a hyperbola on I_{sp}-I_b curve. The equilateral hyperbolas listed in Fig. 7 are the iso-thrust efficiency curves at the stored energy of 10 J and the thrust efficiency of 4.5 %, 5.5 %, 9.0 %, and 11.0 %, respectively. It is considered that the thrust efficiency depends on the cavity diameter, because the plots of the each cavity diameter approximately correspond to each iso-thrust efficiency curves. And it becomes also evident that the higher thrust efficiency was achieved with the smaller cavity diameter.

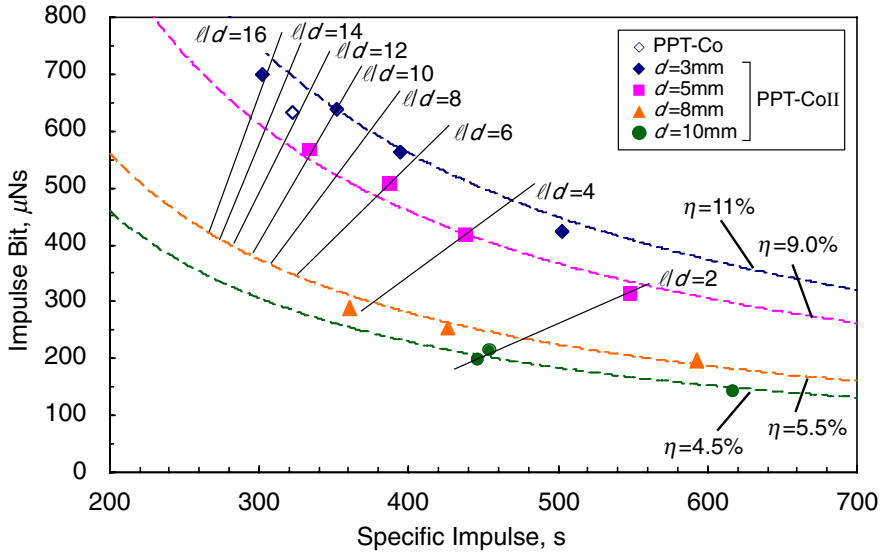

Fig. 7 Thrust performance range with coaxial PPTs (E_0=const=10J).

B. Results of Impulse Bit Range Measurement

B-1. Achieved Impulse Bit Range with Some Cavity Configuration

Figure 8 shows an achieved impulse bit with PPT-Co and PPT-CoII (d =3mm, ℓ =20mm) by varying the stored energy, compared with those of some conventional rectangular PPTs that include PPT-B20[5]. As shown in Fig. 8, it is apparent that the coaxial PPTs generate larger impulse bit than those of the rectangular PPTs at the same stored energy. The maximum impulse bit was 2.5 mNs at the stored energy of 28 J with PPT-Co, and then, the specific thrust (I_b/E_0) achieved 90μN/W. It is approximately 14 times as high as that of PPT-B20 shown in Table 1. As a result, it is considered that the coaxial configuration with Teflon cavity is very appropriate to generate the large impulse bit. Furthermore, a very wide range of the impulse bit, from the minimum value of 3 μNs to the maximum value of 2.5 mNs, was achieved by varying the only stored energy.

And the slight difference of the impulse bit was confirmed between PPT-Co and PPT-CoII, which had the same cavity configuration. The increase of the impulse bit is expected by applying the divergent nozzle, because the differences of the experimental conditions were the divergent nozzle and the capacitors mentioned in a later section.

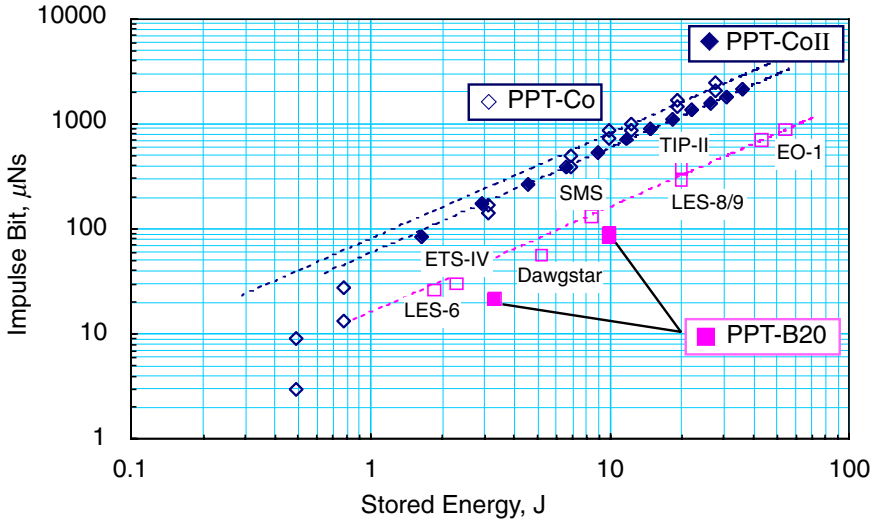

Fig. 8 Impulse bit range with PPT-Co and PPT-CoII (d=3mm, ℓ=20mm) arranged by the stored energy.

B-2. Impulse Bit and Specific Thrust

The impulse bit by varying the cavity configurations and the stored energy is shown in Fig. 9 a), arranged by the energy density. As shown in this figure, it is apparent that the each impulse bit was linearly proportional to the energy density, and the larger impulse bit was achieved with longer cavity length. These results were same as the results shown in Fig. 5 a) and Fig. 6 a). Furthermore it is confirmed that the plots at the same cavity length of 20mm almost correspond to each other. As a result, it is considered that the impulse bit arranged by the energy density depends on the cavity length.

The specific thrust is shown in Fig. 9 b). At the same cavity diameter or length, it is confirmed that the higher specific thrust is also achieved at the higher ℓ/d. Furthermore in Fig. 9 b), it is apparent that the specific thrust decreased at the lower energy density ($E_0/S < 3.0$J/cm^2), although it is nearly constant at the higher energy density. Therefore in addition to the extreme condition indicated in Eq. (4), the condition for a better operation becomes as follows:

$$E_0/S \geq 3.0 \ [J/cm^2] \tag{6}$$

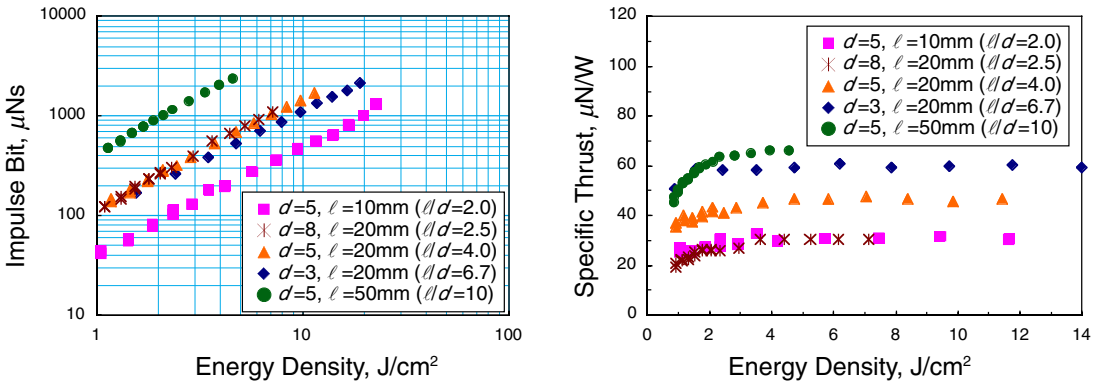

a) Impulse bit b) Specific thrust ($=I_b/E_0$)

Fig. 9 Impulse bit and specific thrust arranged by energy density.

C. Achieved Thrust Performance Range with PPTs in TMIT Lab.

All thrust performance achieved in TMIT Lab. with the coaxial PPTs and the rectangular PPTs are shown in Fig. 10. The coaxial PPTs include PPT-Co and PPT-CoII, and the rectangular PPTs include PPT-B20 and the PPT which propellants are fed from breech and both sides of the electrodes[5]. As a result, a very wide range of the thrust performance has been achieved, and the maximum impulse bit is generated with the coaxial PPT, and the value of it is approximately 1.5 mNs with the specific impulse of 360 s. On the other hand, the maximum specific impulse is obtained with the rectangular PPT, and the value of it is approximately 1900 s with the impulse bit of 90 μNs. In general, the thruster that has the large impulse bit with the low specific impulse is the type of an electrothermal acceleration, and that has the high specific impulse with the small impulse bit is the type of an electromagnetic acceleration. As shown in Fig. 10, it is considered that the coaxial PPTs with Teflon cavity exhibit the characteristics of an electrothermal acceleration, and the rectangular PPTs exhibit those of an electromagnetic acceleration. These wide thrust performance of PPTs is the major advantages for the application to the small satellite.

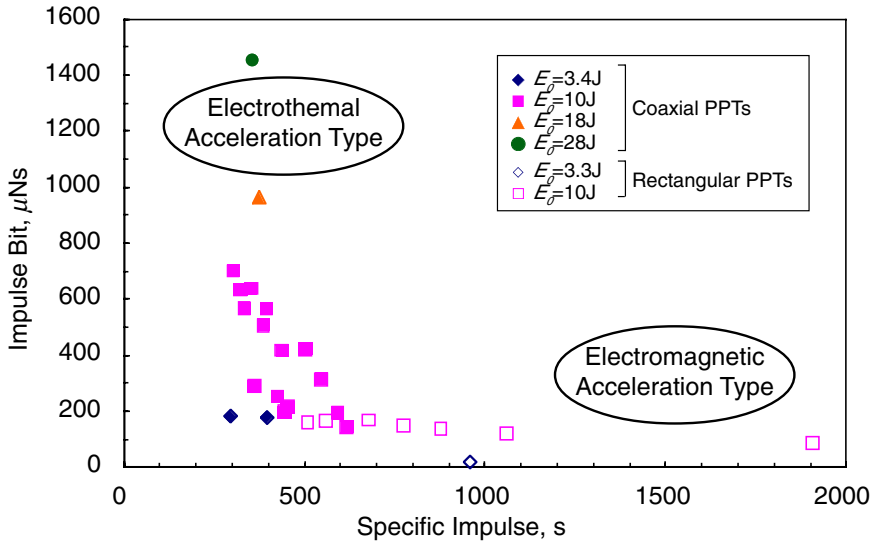

Fig. 10 Achieved thrust performance range with PPTs in TMIT Lab.

D. Analysis of Main Discharge Circuit

D-1. Definition of Initial Resistance and Inductance

In general, the main discharge circuit of the PPT is equivalently expressed as the LCR circuit as shown in Fig. 11. The parameters L, C, R in this figure, indicate the inductance, the capacitance, and the direct-current resistance, respectively. And the subscripts c, p, t indicate the capacitors, the discharge plasma, and the transmission lines including the electrodes, respectively. And L_c and R_c are generally called the equivalent series inductance (ESL) and equivalent series resistance (ESR), respectively. The total inductance L_{tot} and resistance R_{tot} are indicated as follows:

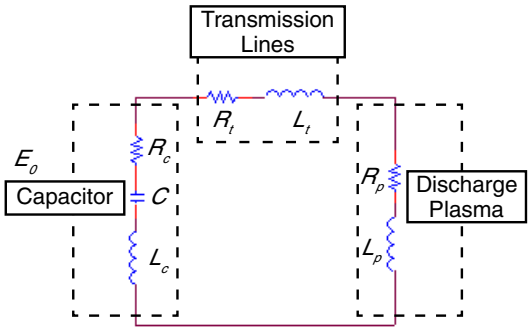

Fig. 11 Equivalent LCR circuit of main discharge.

$$L_{tot} = L_p + L_c + L_t \tag{7}$$

$$R_{tot} = R_p + R_c + R_t \tag{8}$$

In this circuit when the resistance and the inductance are constant during discharge, the following differential equation are obtained[9]:

$$L_0\ddot{Q} + R_0\dot{Q} + \frac{Q}{C} = 0 \tag{9}$$

where Q is the electric charge stored in capacitors, and L_0 and R_0 are the total inductance and resistance at the beginning of the discharge, respectively. In the case of $CR_0^2/4L_0<1$ in Eq. (9), the main discharge current J becomes the damped oscillation, is indicated as Eq. (10). This equation is applicable all current waveforms obtained in this study, because those waveforms exhibited the damped oscillation.

$$J = \frac{V}{\omega L_0} exp[-R_0 t/2L_0] sin\,\omega t \tag{10}$$

where ω is an angular frequency

$$\omega = \sqrt{\frac{1}{L_0 C} - \frac{R_0^2}{4L_0^2}} \tag{11}$$

and t is the time.

At first, the initial values of the inductance and resistance (L_0 and R_0) were defined. Figure 12 shows the typical experimental and the calculated current waveforms with PPT-B20 and PPT-CoII (d =5mm, ℓ =20mm). In this calculation, Eq. (10) and the experimental values were used. As shown in Fig. 12, it is confirmed that the calculated value approximately corresponds to the experimental value in PPT-B20. On the other hand, the difference between those two values is confirmed in PPT-CoII. It is considered that the resistance and the inductance were approximately constant in PPT-B20 during the discharge, while those values were not constant in PPT-CoII. Because Eq. (10) was defined as a constant resistance and inductance. Therefore in order to define the intial inductance and resistance in the coaxial PPTs, the calculated curves were corresponded to the experimental curves in the phase range from 0 to π. The resistance and the inductance were varied as the parameter, the values when the calculated curve correspond to the experimental curve were defined as the initial inductance and resistance, respectively. This approximated curve is shown in Fig. 13 as "by initial conditions".

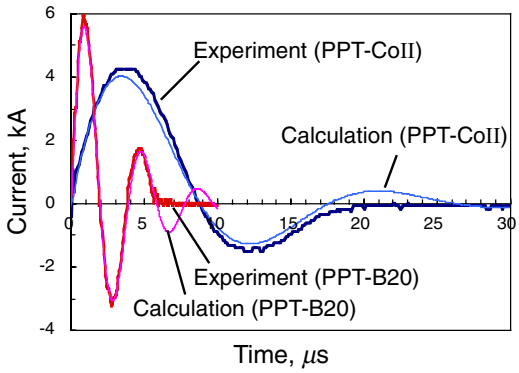

Fig. 12 Experimental and calculated current waveform with PPT-B20 and PPT-CoII (d =5mm, ℓ =20mm).

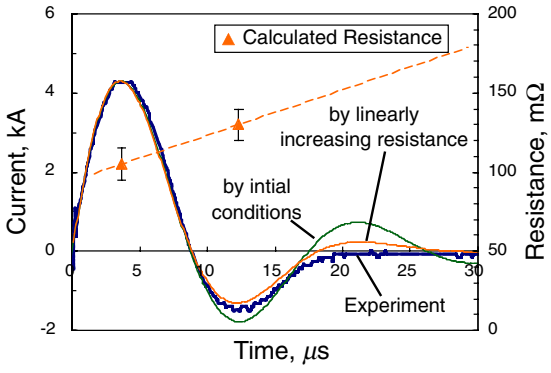

Fig. 13 Approximated current waveforms based on initial conditions and linearly increasing resistance.

D-2. Variation of Circuit Characteristics through Discharge

Next, to investigate the above variation of circuit characteristics through a discharge, the calculated curve was fitted in the phase range from π to 2π. As a result, the inductance was approximately constant compared with the value in the phase range from 0 to π, on the other hand, an increase of the resistance was confirmed as shown in Fig.13. Therefore, it is considered that the resistance in the coaxial PPT with Teflon cavity increases through a discharge. This result was confirmed in the other research institute[10]. Furthermore it was assumed that the resistance was linearly proportional to the time as the dotted line shown in Fig. 13, the approximated curve "by linearly increasing resistance" was also obtained. It is apparent that this approximated curve is closer to the experimental curve than approximated curve "by initial conditions". This variation of the resistance through the discharge affects the joule heating energy of the plasma mentioned in later section. However, in order to simplify the calculation, the initial resistance is applied in this study.

D-3. Influences of cavity configuration on characteristics of main discharge circuit

Figure 14 a) shows the calculated initial inductances by varying the cavity configurations, arranged by the cavity length. As can be seen from this figure, the initial inductances with PPT-CoII were almost constant with increasing cavity length. And this matter represent that the inductance of the plasma L_p is almost constant in each configurations, because it is considered that the inductance L_c+L_t were approximately constant on the angular frequency range of the PPT main discharge[6]. And for the initial inductance with PPT-Co as shown in Fig. 14 a), it is apparent that the value is much lower than that of PPT-CoII. It is considered that the inductance of capacitors makes total inductance low, because the capacitors used in tests with PPT-Co have very low inductance (ESL).

And the calculated initial resistances are shown in Fig. 14 b). As can be seen from this figure, it was confirmed that the resistances was linearly proportional to the cavity length. And the inclination was larger at the smaller cavity diameter. As the low total resistance of PPT-Co, the influence of the resistance of capacitors (ESR) is conceivable as well as the case of the inductances. Furthermore in this figure, the resistance at the cavity length of 0 mm becomes the total resistance (R_c+R_t) except the plasma resistance. Therefore, this value was obtained by averaging the value of each intercept, and the value was approximately 35 mΩ.

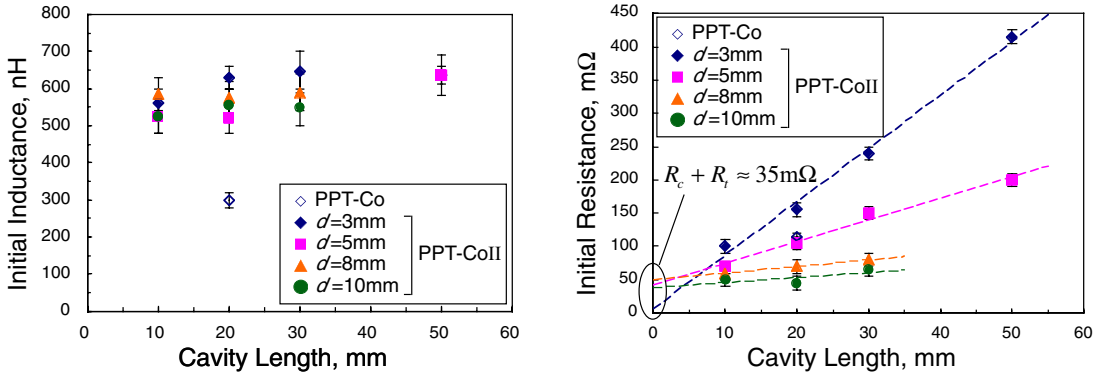

a) Initial inductance arranged by cavity length

b) Initial resistance arranged by cavity length

Fig. 14 Initial characteristics in main discharge circuit by varying cavity configurations (E_0=const=10J).

D-4. Estimation of Energy Distribution

In this section, the energy distribution of the stored energy is estimated. At first, the energy conservation through the discharge is given as follows:

$$E_0 = E_{in} + E_{loss} \tag{12}$$

where E_{in} is the energy supplied to the thruster head, and E_{loss} is the lost energy in each resistor shown in Fig. 11. And the both energy are indicated as follows[6, 9]:

$$E_{in} = \int R_p J^2 dt + \int \frac{\dot{L}_p}{2} J^2 dt \tag{13}$$

$$E_{loss} = \int (R_c + R_t) J^2 dt \tag{14}$$

where the first term in the right side of Eq. (13) is the joule heating energy in the plasma, and the second term is the energy used for the electromagnetic acceleration. From Eqs. (12)-(14), the following equations are obtained:

$$E_{in} = E_0 - \int (R_c + R_t) J^2 dt \tag{15}$$

$$\int R_p J^2 dt = \int R J^2 dt - \int (R_c + R_t) J^2 dt \tag{16}$$

$$\int \frac{\dot{L}_p}{2} J^2 dt = E_{in} - \int R_p J^2 dt \tag{17}$$

Furthermore, the transfer efficiency η_{tr} and the acceleration efficiency η_{acc} are defined as follows[6, 11]:

$$\eta_{tr} = E_{in} / E_0 \tag{18}$$

$$\eta_{acc} = E_t / E_{in} \tag{19}$$

where E_t is the energy utilized to the plasma acceleration, indicated as $E_t = E_0 \times \eta$. And it is considered that the loss in acceleration process includes the wall heating, the frozen flow, the wall drag, the exhaust beam divergence, and the exhaust velocity distribution[10, 11]. To facilitate understanding of above each energy and efficiency, the schematic of the energy distribution is shown in Fig.15.

Figure 16 shows the each energy efficiency and the ratio of joule heating energy to the energy used for the electromagnetic acceleration, at the cavity diameter of 3 mm and the stored energy of 10 J. As shown in Fig. 16, although the thrust efficiency was almost constant, the transfer efficiency improved and the acceleration efficiency deteriorated with the increase of the cavity length, respectively. Furthermore judging from the ratio of joule heating energy to the energy used for the electromagnetic acceleration, it is apparent that the former energy is higher than the latter energy. As mentioned above, the coaxial PPTs with the Teflon cavity represent the characteristics of a large impulse bit with a small specific impulse. Although the energy used for the electrothermal acceleration becomes the amount that subtracts the above losses from the joule heating energy, it was suggested that the coaxial PPT with Teflon cavity was dominated by the electrothermal acceleration in terms of this energy distribution and those thrust performance.

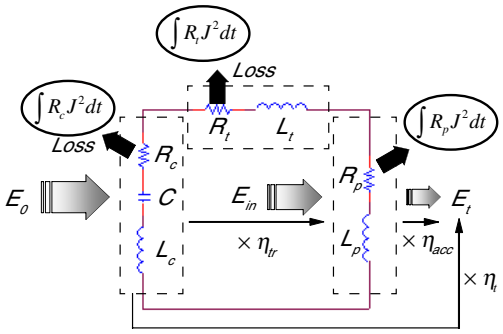

Fig. 15 Schematic of energy distribution.

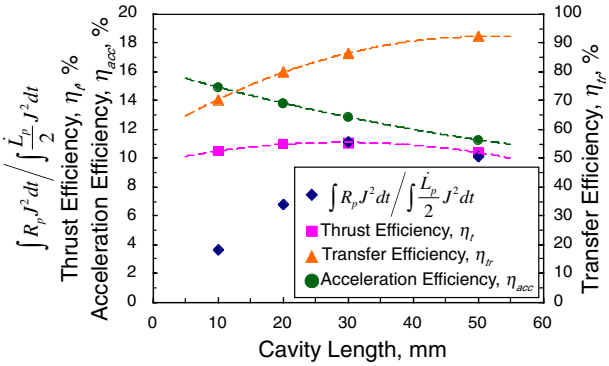

Fig. 16 Energy distribution and each energy efficiency arranged by cavity length (d =3mm, E_0=10J).

V. Conclusions

The coaxial PPT with Teflon cavity was developed to aim the large impulse bit, its thrust performance and characteristics were investigated. The results are:

1) The impulse bit was linearly proportional to the stored energy. Especially with PPT-Co (with divergent-nozzle model), a very wide range of the impulse bit, from the minimum value of 3 μNs at the stored energy of 0.5 J to the maximum value of 2.5 mNs at the stored energy of 28 J, was achieved. On the other hand, the specific impulse and the thrust efficiency were almost constant with the increase of the stored energy.
2) Larger impulse bit with lower specific impulse was generated at smaller cavity diameter and/or longer cavity length. Furthermore, the thrust efficiency almost depended on the cavity diameter, and the higher thrust efficiency was achieved with the smaller cavity diameter.
3) The maximum specific thrust achieved 90 μN/W with the coaxial PPT, it became evident that the coaxial configuration with Teflon cavity is very appropriate to generate the large impulse bit.
4) In addition to the rectangular PPTs that have been reseached in TMIT, the PPT that generates larger impulse bit was established with almost same dimension (approximately 50×50×100 mm), weight (less than 2 kg), and power consumption (less than 30 W). By using these PPTs, a very wide range of the thrust performance, from the impulse bit of 1.5 mNs with the specific impulse of 360 s to the impulse bit of 90 μNs with the specific impulse of 1900 s, were achieved.

5) As the parameter to estimate the energy distribution, each energy and each energy efficiency were defined. In terms of this each energy and those thrust performance, it is suggested that the coaxial PPT with Teflon cavity was dominated by the electrothermal acceleration.

Acknowledgement

The authors would like to express their sincere thanks to Dr. Kuriki K., a guest professor of Tokyo Metropolitan University, who has given very significant advices in going ahead with our study.

References

[1]R. L. Burton, and P. J. Turchi, "Pulsed Plasma Thruster," *Journal of Propulsion and Power*, Vol.14, No.5, 1998, pp. 716-735.

[2]Kumagai, N., Sato, K., Tamura, K., Kawahara, K., Koide, T., Takegahara H., et al., "Research and Development Status of Low Power pulsed Plasma Thruster System for μ-Lab Sat II," 28th International Electric Propulsion Conference, Toulouse, France, IEPC-03-0202, 2003.

[3]Iio, J., Uezu, J., Fukushima, T., Kamishima, Y., and Takegahara, H., "Evaluation on Impulse Bit Characteristics of Pulse Plasma Thruster by Single Impulse Measurement," 29th International Electric Propulsion Conference, Princeton, USA, IEPC-05-236, 2005.

[4]Fukushima, T., Kawahara, K., Koide, T., Uezu, J., Iio, J., Takegahara, H., et al., "R&D on Pulsed Plasma Thruster for μ-Lab Sat II -Development Status of EM-," 24th International Symposium on Space Technology and Science, Miyazaki, Japan, ISTS-b-05, 2004.

[5]Kamishima, Y., Fukushima, T., Uezu, J., Iio, J., and Takegahara, H., "Study on Impulse Bit Increase by Modification of PPT Configuration," 56th International Astronautical Congress, Fukuoka, Japan, IAC-05-C4.P.02, 2005.

[6]Edamitsu, T., Tahara, H., and Yoshikawa, T., "Performance Characteristics of a Coaxial Pulsed Plasma Thruster with Teflon Cavity," Asian Joint Conference on Propulsion and Power, Seoul, Korea, pp. 324-334, 2004.

[7]Kameoka, M., Takegahara H., Shimizu Y., Toki, K., "Single Impulse Measurement of a Coaxial Pulsed Plasma Thruster," 28th International Electric Propulsion Conference, Toulouse, France, IEPC-03-0093, 2003.

[8]Rysanek, F., and Burton, R. L., "Effects of Geometry and Energy on a Coaxial Teflon Pulsed Plasma Thruster," AIAA Paper No. 2000-3429, July, 2003.

[9]Kuriki, K., and Arakawa, Y., *Introduction to Electric Propulsion*, University of Tokyo Press, Tokyo, 2003, pp. 157-181. (in Japanese)

[10]Rysanek, F., and Burton, R., "Performance and Heat Loss of a Coaxial Teflon Pulsed Plasma Thruster," 27th International Electric Propulsion Conference, Pasadena, California, USA, IEPC-01-151, 2001.

[11]Michael, M., and Andrew, D., *Micropropulsion for Small Spacecraft*, American Institute of Aeronautics and Astronautics, Virginia, 2001, pp. 337-352.